Use of Different Size Grids to Control the Surface Chemistry of Plasma-Polymerized Acrylic Acid Films in a Hybrid Discharge

Marshal Dhayal

Biological Research Center of Industrial Accelerators, Dongshin University, 252 Daeho-Dong, Naju, Chonnam, South Korea

Received 13 January 2006; accepted 4 September 2006
DOI 10.1002/app.25471
Published online in Wiley InterScience (www.interscience.wiley.com).

ABSTRACT: The surface chemistry of plasma-polymerized acrylic acid (ppAc) films were controlled in a two-stage (primary and processing) hybrid radio frequency (RF) discharge by changing the grid wire spacing (d_s). Two regions were defined in terms of d_s with respect to Debye length (λ_d) in the primary chamber at the grid to control the electron temperature (T_e) and surface chemistry of the ppAc films deposited in the processing chamber. A higher T_e (>3 eV) in the processing plasma was possible for $d_s > \lambda_d$, whereas decreasing d_s relative to λ_d reduced T_e. X-ray photoelectron spectroscopy was used to characterize the ppAc films deposited on a glass substrate. The ppAc films surface characterization showed the maximum proportion of carbon atoms as carboxylic/ester [C(=O)OX] functionalities in C1s at the surface of films for the grid with $d_s \approx \lambda_d$. The proportion of carbon atoms as —[C(=O)OX] and COX in C1s at the surface decreased when d_s decreased relative to λ_d. The proportion of carbon atoms as carbonyl (C=O) at the film surface showed very good stability for all of the d_s values explored in this study. © 2007 Wiley Periodicals, Inc. J Appl Polym Sci 104: 2219–2224, 2007

Key words: biomaterials; coatings; ESCA/XPS; films; functionalization of polymers

INTRODUCTION

For many years, the plasma polymerization process for thin-film deposition has been the subject of intensive research efforts. This is because plasma polymerization has advantages in providing good adhesion to the substrate and pin-hole-free, mechanical, and chemical stability to the films.[1–18] In these plasma polymerization processes, the variation of external discharge parameters, such as the pressure, flow rate, and effective power for both the continuous and pulsed modes, are used to control the surface properties of the films.[2–6] The research has indicated that in low-pressure RF (13.56 MHz) discharges, films have a high degree of chemical functionality of the monomer if they were deposited at low effective powers in both continuous[7] and pulsed modes.[8,9]

In the past few years, the use of pulsed radio frequency plasmas has become important in the deposition of polymeric films, and the duty cycle has been reported as a key parameter in the determination of the retention of the chemical nature of the monomer in the deposited films.[3,4] The use of a pulsed RF discharge to achieve a higher selectivity in the surface chemistry of the polymeric films is quite popular, but the presence of higher energetic electrons (ions) at the start of each pulse[19] in the discharge may damage the structure of the surface. However, we used a two-stage hybrid discharge for acrylic acid plasma polymerization to deposit films with a higher degree of original monomer retention, and it had low-energy ions/electrons in the discharge.[1,11,20–22]

This process is particularly important for the coatings on micro/nano devices [micro/nano-electromechanical systems (MEMS/NEMS)] because the use of pulse plasma polymerization can possibly damage the microstructure or nanostructure of the electrodes patterned on these devises due to higher energetic electrons (ions) at the start of each pulse. Therefore, in these applications, a hybrid plasma polymerization process with low electron (ion) energy could have advantages for the deposition of polymeric films with the control of surface chemistry.[1,11,20]

In this study, the effects of variation in the grid wire spacing (d_s) in a two-stage hybrid plasma polymerization process to control the surface chemistry of films was investigated. Grids with five different d_s values (G1, G2, G3, G4, and G5) were used in this study. Films were deposited at a constant pressure,

Correspondence to: M. Dhayal, Liquid Crystal and Self Assembled Monolayer Section, Engineering Material Division, National Physical Laboratory, Dr KS Krishnan Marg, New Delhi 110012, India (marshaldhayal@yahoo.com).

Contract grant sponsor: Biology Research Center of Industrial Accelerators, Dongshin University.

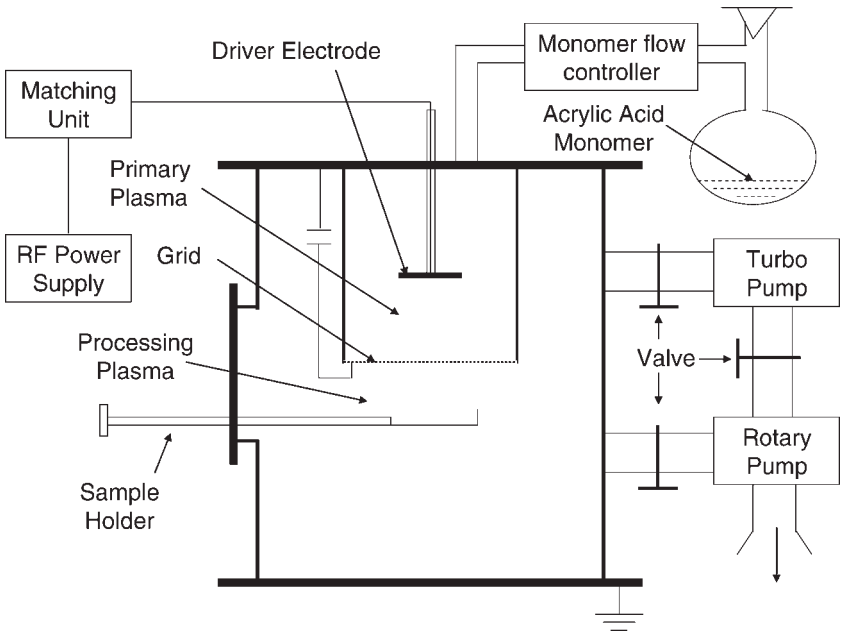

Figure 1 Schematic diagram of the two-stage plasma polymerization reactor.

power, and monomer flow rate for all of the different size grids. The wire diameters of these grids were 0.03, 0.053, 0.18, 0.23, and 0.4 mm, and the spacings between these grid wires were 0.03, 0.1, 0.33, 0.62, and 1.72 mm, respectively, for grids G1, G2, G3, G4, and G5.

In grids G1, G2, and G3, the d_s value was less than the Debye length (λ_d), and the electron temperature (T_e) in the processing discharge was less than 1 eV. For grids G4 and G5, d_s was greater than λ_d, and T_e was about 3 eV.[11,23] In this study, a constant pressure of 40 mTorr, a constant RF power of 20 W, and a constant sample position at 70 mm from the grid was used for all of the experiments.

EXPERIMENTAL

A schematic diagram of a two-stage plasma polymerization reactor is shown in Figure 1. This two-stage plasma reactor was made from a four-way cruciform stainless steel vessel (diameter = 180 mm) and was pumped to a base pressure on the order of 10^{-5} torr with a turbomolecular pump backed by a rotary pump. The main plasma was sustained through 13.56 MHz RF excitation in the main plasma region, which consisted of a 150 mm long and 120 mm diameter stainless steel cylinder mounted on one side of the flange of the diffusion region. The RF driver electrode was a Cu plate 80 mm in diameter attached to the RF power supply via a matching unit. The matching unit could be operated in two modes. First, it could be operated automatically for argon gas, and for other gases or monomer vapors, it could also be tuned manually to control the reflected power, and it was less than 5%. The RF power supply range was 0–200 W, and in this study, a constant power (20 W), pressure (40 mTorr), and flow rate were used. Different sizes of circular grids 80 mm in diameter and made of stainless steel were used. The grids were attached to the ground via a 10 μF capacitor to null RF excitation on the mesh due to RF power in the primary discharge; a detailed description of the operation has been discussed elsewhere.[11,20–25]

The acrylic acid monomer was contained in glassware mounted on one flange of the reactor through a microleveler manually controlled gas flow regulator. The acrylic acid monomer was degassed with a freeze–thaw cycle four times before it was admitted to the chamber for the discharge. An oxygen gas line was attached to the chamber through a gas flow controller system to the reactor and used to clean the reactor after each set of deposition experiments. The surface characterization of plasma-polymerized acrylic acid (ppAc) films was carried out with X-ray photoelectron spectroscopy (XPS). In this study, XPS was performed with a VG-Scientific ESCALAB 250 spectrometer with a monocromatized Al Kα X-ray source (Korean Basic Science Institute, Korea).

In this type of discharge, the control of the diffusion of energetic electrons from the primary chamber to the process chamber through the grid is a key parameter in the control the surface chemistry of the depositing films. This is because the control of the flux of these energetic electrons diffused from primary discharge can be changed by variation of

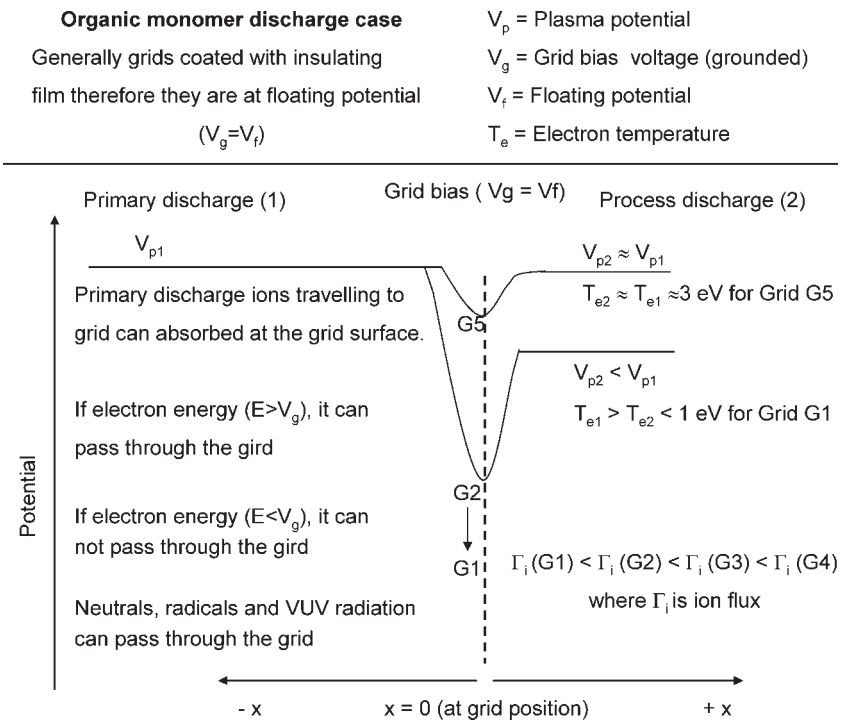

Figure 2 VUV is the vacuum ultra violet radiation. Schematic diagram of the two-stage plasma polymerization process (Γ_i = ion flux).

the grid bias voltage or grid size; therefore, one can control plasma chemistry in the process chamber by changing d_s. A schematic diagram is shown in Figure 2 to demonstrate the discharge processes. The energetic electrons diffused from the primary chamber can release their energy in collisions with the neutrals to sustain secondary discharge in the process chamber. The effect of different size grids on the plasma parameter in the plasma chamber for argon gases were also reported by Hong et al.[23] A decrease in d_s can decrease the electron flux and increase the ratio of higher energetic electrons[23] in the plasma process.

T_e and plasma density (N_e) were measured for grid G2[11,20] for different powers and distances from the grid in the processing chamber for acrylic acid plasma. The values of T_e and N_e were on the order of about 1 eV and about 5×10^{13} m^{-3}, respectively. A higher T_e ($\geq$3 eV) in the process chamber (similar to the primary discharge conditions) was possible for d_s by more than λ_d at the grid in the primary chamber, whereas a decrease in d_s could lower T_e ($\leq$1 eV) in the processing discharge. In the discharge, an approximate λ_d at the grid wire was determined by the primary plasma parameter. For the current operating conditions, N_e and T_e had values on the order of about 10^{15}–10^{16} m^{-3} and 3–5 eV, respectively, in the main discharge and depended on the discharge pressure and power. Therefore, λ_d was approximately 0.4–0.5 mm at the grid for these operating conditions. In terms of d_s and λ_d in the primary chamber, two regions were defined to control the surface chemistry of the thin plasma-polymerized films. The first region, (region 1) was associated with d_s values of less than 0.4 mm (grids G1, G2, and G3) and low T_e values ($\leq$1 eV), and the second region (region 2) was associated with d_s values greater than 0. 5 mm and higher T_e values ($\geq$3 eV; grids G4 and G5) in the processing plasma.

The variation of d_s only changed the plasma parameters in the processing chamber, but the primary discharge parameters remained approximately constant for all grid sizes for constant pressure and power conditions. In this two-stage discharge, the interface between the primary plasma and the processing chamber can be described in two parts: the grid wire area (the physical grid wire area) and the grid-wire-free region. The grid-wire-free area (the optical transmission) and d_s in different used grids played an important role in the control of the diffusion of electrons and neutrals from the primary plasma.

The deposition rate (DR) for different grids was measured and correlated with relatively wire-free areas of the grid (or the optical transmission of the grid). Figure 3 shows a plot of DR and optical transmission of the grid with d_s. The optical transmission of the grids increased with increasing d_s, whereas variation in DR with d_s showed two characteristics in terms of d_s and λ_d. In region 1 ($d_s < \lambda_d$), DR

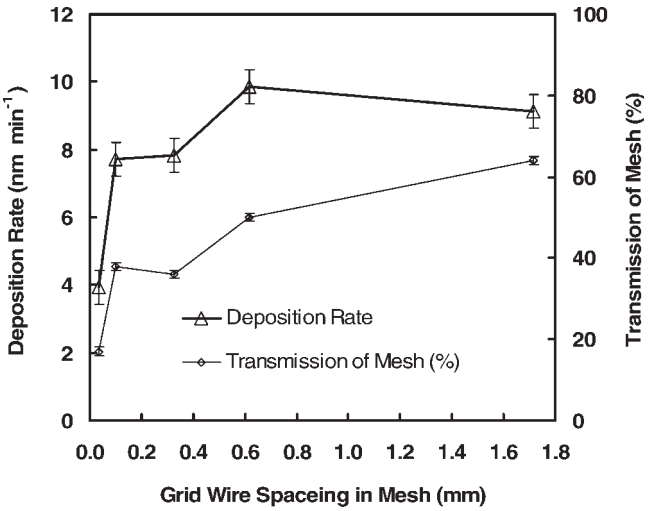

Figure 3 Optical transmission and DR measurements with d_s at a constant pressure of 40 mTorr, RF power of 20 W, and 70 mm from the grid.

increased with increasing d_s, and in region 2 ($d_s > \lambda_d$), a small reduction was observed with a further increase in d_s.

RESULTS AND DISCUSSION

The change in the surface chemistry of the films in the two-stage plasma polymerization process with grid size spacing was characterized by XPS. A peak-fitted narrow-scan C1s XPS spectrum of the ppAc film deposited on the glass substrate with grid G1 (the grid with minimum grid wire spacing) is shown in Figure 4. This C1s spectrum was fitted with six peaks, and the chemical shift relative to the C—Si peak is quoted in parentheses: C—Si at 283.7 eV (0 eV), hydrocarbon (C—H/C—C) at 286 eV (2.3 eV), C—C(=O)OX at 286.5 (2.8), alcohol/ether (C—OX) at 287.5 eV (3.8 eV), carbonyl (C=O) at 288.8 eV (5.1 eV), and carboxylic/ester [C(=O)OX] at 290.2 eV (6.5 eV). Generally, in plasma polymerization of acrylic acid films, C—C/C—H, C—OX, C=O, and C(=O)OX peaks are observed in the C1s narrow-scan XPS spectrum. However, in this study, an additional peak toward lower binding energy in the C1s XPS spectrum was also measured.

Figure 5 shows the peak-fitted narrow-scan C1s spectrum of the ppAc film deposited with grid G3 ($d_s \approx \lambda_d$). This C1s spectrum could also be fitted with six components similar to those shown in Figure 4. The chemical shift relative to the C—Si peak is quoted in parentheses: C—Si at 283.6 eV (0 eV), hydrocarbon (C—H/C—C) at 286.0 eV (2.4 eV), C—C(=O)OX at 286.4 (2.8), alcohol/ether (C—OX) at 287.4 eV (3.8 eV), carbonyl (C=O) at 288.7 eV (5.1 eV), and carboxylic/ester [C(=O)OX] at 290.1 eV (6.5 eV).

The variation in the percentage of carbon atoms as COX, C(=O)OX, and C=O in the C1s XPS spectrum

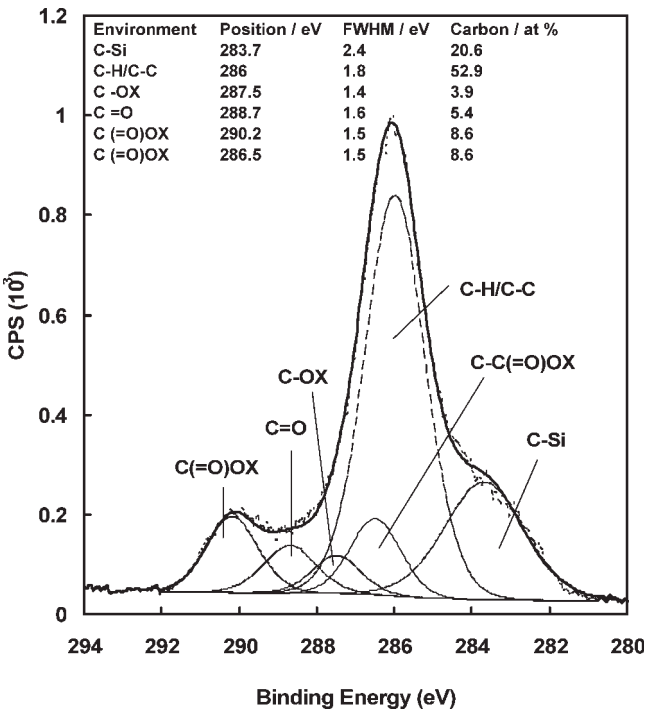

Figure 4 Peak-fitted XPS narrow-scan C1s spectrum of the ppAc film deposited with grid G1 at a pressure of 40 mTorr, RF power of 20 W RF, and 70 mm from the grid. CPS is count per second and FWHM is full width and half maxima of the spectrum.

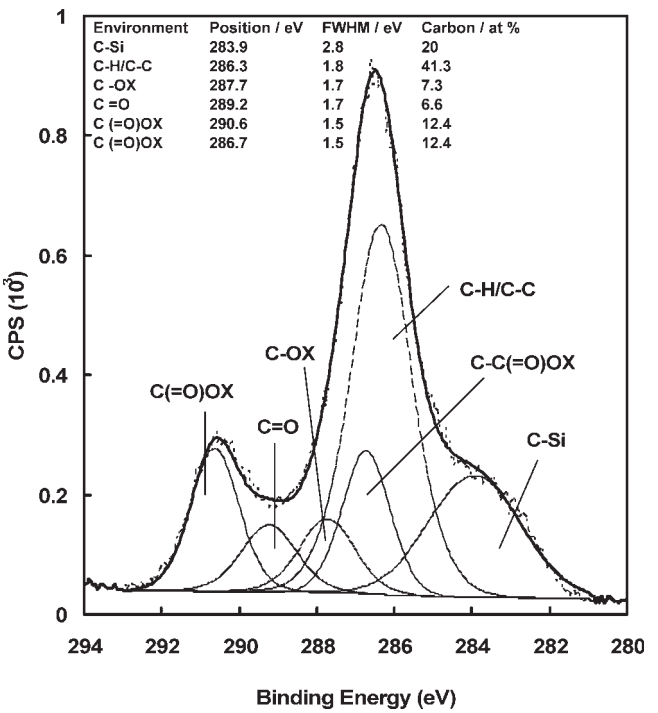

Figure 5 Peak-fitted XPS narrow-scan C1s spectrum of the ppAc film deposited with grid G3 at a pressure of 40 mTorr, RF power of 20 W, and 70 mm from the grid. CPS is count per second and FWHM is full width and half maxima of the spectrum.

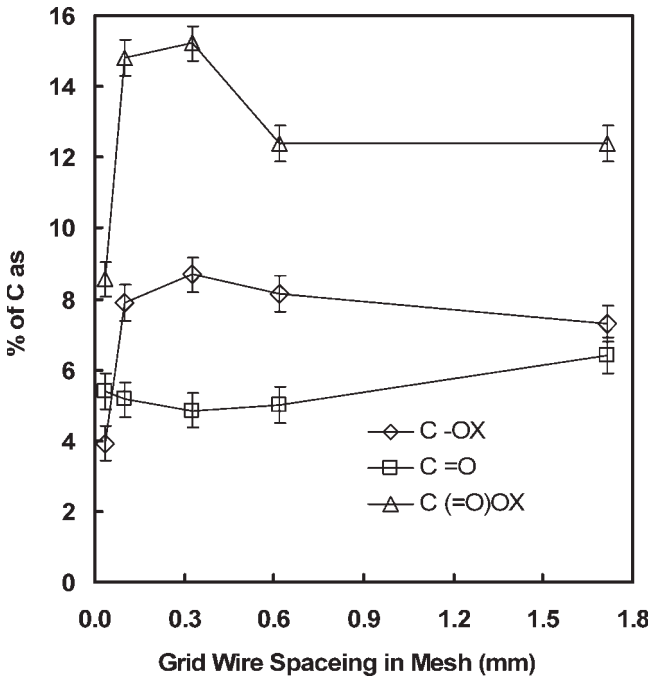

Figure 6 Proportion of carbon atoms present as C—OX (hydroxyl/ether), C(=O)OX (ester/carboxylic), and C=O (carbonyl) functionalities with d_s at a pressure of 40 mTorr, RF power of 20 W, and 70 mm from the mesh.

of the ppAc films was plotted with d_s and is shown in Figure 6. Initially, a rapid increase in the percentage proportion of carbon atoms as COX and C(=O)OX in C1s with d_s was measured. A maximum value was achieved for grid G3 ($d_s \leq \lambda_d$). A decrease in the percentage proportion of carbon atoms as COX and COOX in C1s was measured with further increases in d_s and remained approximately constant for the G4 and G5 grids.

These results show a change in the surface chemistry associated with two regions (classified in terms of λ_d) for grids G1–G5. The percentage proportion of carbon atoms as COX and COOX in C1s strongly depended on d_s in the first region ($d_s < \lambda_d$), whereas in the second region ($d_s > \lambda_d$), no significant change in the surface chemistry was observed. The maximum percentage proportion of carbon atoms as original monomer functionality [—C(=O)OX] in C1s at the film surface was achieved for a grid size that had a d_s value equal to or slightly lower than λ_d at the grid in the primary discharge. Hong et al.[23] showed that a decrease in d_s can decrease the electron flux and increase the ratio of higher energy electrons in the processing plasma for argon plasma. Therefore, a reduction in the DR with decreasing d_s can be associated with electron flux of diffused energetic electrons from the primary plasma. The decrease in COX and COOX functionalities can be associated with an increased ratio of higher energy electrons (diffusing from the primary plasma) in the process chamber.

Another interesting result was the lack of change in the percentage proportion of carbon atoms as C=O in C1s with d_s variation. This indicated that the carbon atoms as C=O in the discharge were quite stable for the variation of T_e from 3 to 1 eV or less. This could be explained as follows: when collisions between energetic electrons (e^-) and monomers ($CH_2CHCOOH0$ took place in the process chamber, there was a higher probability of single-bond breaking in the monomer chain (CH_2CH—COOH or CH_2CHCO—OH) that could lead to the generation of —COOH and —OH radicals in the discharge, whereas the possibility of carbon–oxygen double-bond breaking in the monomer [CH_2CHC(OH)=O] was small due to the higher bond energy of C=O double bonds relative to single bonds. Breaking the double bond (C=O) required more energy, possibly beyond the range of energy in this discharge for all d_s values. It was possible to have an approximately constant proportion of carbon atoms as C=O in C1s for all of d_s values explored in this study. Therefore, the proportion of carbon atoms as C=O in the discharge was more stable with the variation of T_e with changing d_s, whereas the proportion of carbon atoms as C(=O)OX and COX was very sensitive in the discharge with the discharge parameters.

CONCLUSIONS

It was possible to control the surface chemistry of ppAc films with the variation of d_s in a two-stage hybrid RF discharge. Two regions were identified in terms of d_s and λ_d at the grid in the primary discharge to control the surface chemistry of the thin plasma-polymerized films. The maximum proportion of carbon atoms as original monomer functionalities in the ppAc films was achieved for a d_s value that was equal to λ_d or less. A decrease in the percentage proportion of carbon atoms as carboxylic/ester and hydroxyl/ether in C1s at the surface of the films was observed with a decrease in d_s relative to λ_d at the grid. The percentage proportion of carbon atoms as carbonyl functionalities in C1s at the film surface remained approximately constant for all different d_s values. This indicated that the carbonyl functionality in the discharge was more stable with the variation of T_e values associated with different d_s values, whereas carboxylic/ester and hydroxyl/ether functionalities were very sensitive in the discharge with the discharge parameters.

The author thanks Dr. M.K. Ha (Korean Basic Science Institute) for assistance in obtaining the XPS spectrum. The author also thanks Sarah Morgan from Manchester University, England, for her comments on the English.

References

1. Dhayal, M. J Vac Sci Technol A 2006, 24, 1751.
2. Yasuda, H. Plasma Polymerisation; Academic: London, 1985.
3. Rinsch, C. L.; Chen, X.; Panchalingam, V.; Eberhart, R. C.; Wang, J. H.; Timmons, R. B. Langmuir 1996, 12, 2995.
4. Han, L. M.; Timmons, R. B.; Bogdal, D.; Pielichowski, J. Chem Mater 1998, 10, 1422.
5. Leich, M. A.; Mackie, N. M.; Williams, K. L.; Fisher, E. R. Macromolecules 1998, 31, 7618.
6. Ryan, M. E.; Hayes, A. M.; Badyal, J. P. S. Chem Mater 1996, 8, 37.
7. Limb, S. J.; Gleeson, K. K.; Edell, D. J.; Gleason, E. F. J Vac Sci Technol A, 1997, 15, 1814.
8. Wang, J. H.; Chen, J. J.; Timmons, R. B. Chem Mater 1996, 8, 2212.
9. Alexander, M. R.; Duc, T. M. J Mater Chem A 1998, 8, 937.
10. Labelle, C. B.; Gleason, K. K. J Vac Sci Technol A 1999, 17, 445.
11. Dhayal, M. PhD Thesis, University of Manchester Institute of Science and Technology, Manchester, England, 2003.
12. Haddow, D. B.; Beck, A. J.; France, R. M.; Fraser, S.; Whittle, J. D.; Short, R. D. J Vac Sci Technol A 2000, 18, 3008.
13. Fraser, S.; Barton, D.; Short, R. D.; Bradley, J. W. J Phys Chem B 2002, 106, 5596.
14. Guerin, D. C.; Hinshelwood, D. D.; Monolache, S.; Denes, F. S.; Shamamian, V. A. Langmuir 2002, 18, 4118.
15. Barton, D.; Bradley, J. W.; Steele, D. A.; Short, R. D. J Phys Chem B 1999, 21, 4423.
16. Spatenka, P.; Endres, H. J.; Krumeich, J.; Cook, R. W. Surf Coat Technol 1999, 116–119, 1228.
17. Yamaguchi, S.; Sawa, G.; Ieda, M. J Appl Phys 1977, 48, 2363.
18. Henry, D.; Jan, M.; Treguier, J. P.; Vuillermoz, B. Phys Lett A 1974, 50, 113.
19. Dhayal, M.; Bradley, J. W. Surf Sci Technol 2005, 194, 167.
20. Dhayal, M.; Bradley, J. W. Surf Coat Technol 2004, 184, 116.
21. Dhayal, M.; Jeong, H. G.; Choi, J. S. Appl Surf Sci 2005, 252, 1710.
22. Dhayal, M.; Alexander, M. R.; Bradley, J. W. In 46th Technical Conference Proceedings of the Society of Vacuum Coaters, San Francisco, 2003; p 93.
23. Hong, J. I.; Seo, S. H.; Kim, S. S.; Yoon, N. S.; Chang, C. S.; Chang, H. Y. Phys Plasma 1999, 6, 1017.
24. Dhayal, M.; Forder, D.; Short, R. D.; Bradley, J. W. Vacuum 2003, 70, 67.
25. Dhayal, M.; Forder, D.; Short, R. D.; Barton, D.; Bradley, J. W. Surf Coat Technol 2003, 162, 294.